The Role of Anomalously Warm Sea Surface Temperatures on the Intensity of Hurricane Juan (2003) during Its Approach to Nova Scotia

CHRISTOPHER T. FOGARTY, RICHARD J. GREATBATCH, AND HAROLD RITCHIE

Department of Oceanography, Dalhousie University, Halifax, Nova Scotia, Canada

(Manuscript received 17 February 2005, in final form 29 June 2005)

ABSTRACT

When Hurricane Juan tracked toward Nova Scotia, Canada, in September 2003, forecasters were faced with the challenge of predicting the intensity and timing of the hurricane's landfall. There were two competing factors dictating the storm's intensity: 1) the decreasing sea surface temperatures (SSTs) over which the hurricane tracked that were conducive to weakening; and 2) the increased forward motion of the storm that enhanced the surface winds on the right (storm relative) side of the storm. Since Hurricane Juan was moving very quickly (forward speed approximately 15 m s^{-1}) it spent less time over the cooler continental shelf waters between Nova Scotia and the >26°C water of the Gulf Stream than would have been the case for a slower-moving storm. However, those waters were warmer than normal during this event, by ~4°C. It is argued that these warmer SSTs made a significant contribution (among other factors) to this rare category-2 hurricane at landfall in Nova Scotia. To assess the role of SSTs on the decay rate of Hurricane Juan, the Mesoscale Compressible Community model of the atmosphere is used. The model consists of a fixed, nested 3-km grid driven by a coarser 12-km grid, and is initiated using a synthetic hurricane vortex constructed from observational information such as storm size and intensity, thus giving a decent representation of the real storm. The model is initiated at 0000 UTC 28 September, when the hurricane was close to maximum intensity. An ensemble of experiments are conducted for each of two SST configurations: 1) analyzed SST of 28 September 2003 and 2) climatological SST representative of late September. Results from the 3-km simulations indicate that the intensity of Hurricane Juan's maximum surface wind just prior to landfall was ~5 m s^{-1} (±~1.5 m s^{-1}) weaker in the normal SST case, a result that is statistically significant at the 99% level. The destructiveness of the maximum landfall winds in the normal SST case is generally about 70% of that in the observed (warmer than normal) SST case. Model performance is measured using surface weather data, as well as data collected from a research aircraft that flew into the storm just prior to landfall.

1. Introduction

a. Overview

When Hurricane Juan struck Nova Scotia, Canada (~44°N latitude), in September 2003 as a category-2[1] storm on the Saffir–Simpson hurricane scale (Simpson and Riehl 1981), most people were surprised by the intensity of the storm and the damage it caused. Millions of trees were blown down, there were widespread power outages, boats were strewn ashore by surge and waves, roofs were torn off buildings, and billboard signs were destroyed. The likes of such damage had not been seen since Hurricane Edna (Malkin and Holzworth 1954) hit the same area in 1954 (see Nova Scotia Department of Natural Resources Web site online at http://www.gov.ns.ca/natr/juan/).

As Hurricane Juan moved northward, it experienced much warmer than normal sea surface temperatures (SSTs) south of Nova Scotia (3° to 5°C above normal) on the Scotian Shelf. Our primary purpose here is to assess the role of these warmer SSTs on the weakening rate of Juan leading up to landfall. Most of the hurricanes that move toward Nova Scotia weaken to cat-

[1] The accepted definition for hurricane intensity in the Atlantic Ocean is based on the maximum 1-min mean winds anywhere in the storm measured or estimated 10 m above the surface (hereafter referred to as "maximum sustained winds").

Corresponding author address: Dr. Christopher Fogarty, Department of Oceanography, Dalhousie University, 1355 Oxford St., Halifax, NS B3H 4J1, Canada.
E-mail: chris.fogarty@ec.gc.ca

egory-1 or tropical storm strength. There have only been three documented cases of category-2 hurricanes making *direct* landfall in Nova Scotia [based on data from the North Atlantic hurricane database available online at http://www.aoml.noaa.gov/hrd/hurdat/easyhurdat_5102.html] in the 150-yr period from 1853 to 2003 (Juan in 2003, Ginny in 1963, and an unnamed storm near Yarmouth, Nova Scotia, in 1891). However, extreme tropical cyclone–related wind events in Nova Scotia are not limited to these three cases. For example, Hurricane Edna made landfall in eastern Maine as a strong category-1 hurricane, yet was responsible for an intense wind jet well east of the storm center over Nova Scotia, delivering winds that inflicted damage similar to Hurricane Juan.

b. Background

There has been a significant amount of work over the years studying the role of SSTs on hurricane intensity (e.g., Emanuel 1988; Evans 1993; DeMaria and Kaplan 1994; Schade 2000), but most of these studies focused on the part of the ocean where SSTs are 26°C or more. A growing community of research has come about in the past decade investigating changes in hurricane intensity at higher latitudes where SSTs are cooler, environmental wind shears are stronger, and where storms move much faster than in the Tropics. Most of this work is conducted in the context of extratropical transition (ET; Jones et al. 2003) whereby a tropical cyclone (TC) moves into the midlatitudes and evolves into an extratropical cyclone. These studies have focused primarily on the synoptic-scale processes associated with ET. Much less is known about structural changes in the wind field of a storm as it accelerates and moves over cooler water, be it a TC undergoing ET, or one that is accelerating and weakening over cool water in the relative absence of atmospheric baroclinicity. In addition, our understanding of decoupling of high winds above the boundary layer (BL) from those within the BL over cooler SSTs needs further investigation. These situations can result in very strong low-level wind shears as documented by Abraham et al. (2004) in Hurricane Michael. In this paper we note some of the changes in the structure of Hurricane Juan as it accelerated and moved over the cooler water when we compare the numerical experiments with surface weather/aircraft data collected during the storm. We hope to gain some understanding that could be very helpful for meteorologists forecasting these storms.

Numerical weather predictions for Hurricane Juan were quite poor during the event. The most common source of these poor predictions was insufficient representation of the hurricane in the model initial conditions. In the Canadian Global Environmental Multiscale model, Juan only appeared as a weak ~1008-hPa low south of Nova Scotia that moved in the wrong direction toward the north-northwest, crossing the western end of the province. Simple insertion of a synthetic TC vortex into the large-scale analysis helps to greatly improve the numerical simulation/prediction of the storm (McTaggart-Cowan et al. 2006b).

We have organized this paper as follows: section 2 describes the synoptic history of Hurricane Juan; section 3 describes the modeling system used to conduct the experiments. In section 4 we present the results from two control simulations, one that uses climatological SST for late September at the lower boundary and the other a realistic SST for the period immediately prior to Juan. The results are compared with surface weather and aircraft data, and in section 5, their robustness is verified using two ensembles of experiments generated using slightly different initial conditions. A summary of the results and conclusions appears in section 6.

2. Synoptic history of Hurricane Juan

The original cyclone that eventually became Hurricane Juan formed approximately 600 km southeast of Bermuda on 23 September 2003. This cyclone formed in a slightly baroclinic environment as an upper-level trough approached a low-level potential vorticity anomaly that had originally formed off the African coast many days earlier. A detailed analysis of the vorticity anomaly associated with the origins of Hurricane Juan is described by McTaggart-Cowan et al. (2006a). A series of satellite images documenting the life cycle of Juan appears in Fig. 1 and the storm track with SSTs appears in Fig. 2. On 24 September, deep convection consolidated near the cyclone center and the system was declared a tropical depression. The cyclone reached tropical storm status by 0000 UTC 25 September. The cloud pattern continued to organize and the cyclone developed an eye, becoming a hurricane by 1200 UTC 26 September (Fig. 1c).

Juan gradually intensified and reached its peak intensity with maximum sustained winds of 46 m s^{-1} (90 kt), and a minimum pressure of 969 hPa, at 1800 UTC 27 September (between the times shown in Figs. 1e,f). Juan moved in a northward direction, embedded in a large tropical air mass over the western Atlantic Ocean. The hurricane gradually accelerated and made landfall west of Halifax, Nova Scotia, near the community of Prospect at 0310 UTC 29 September 2003 with esti-

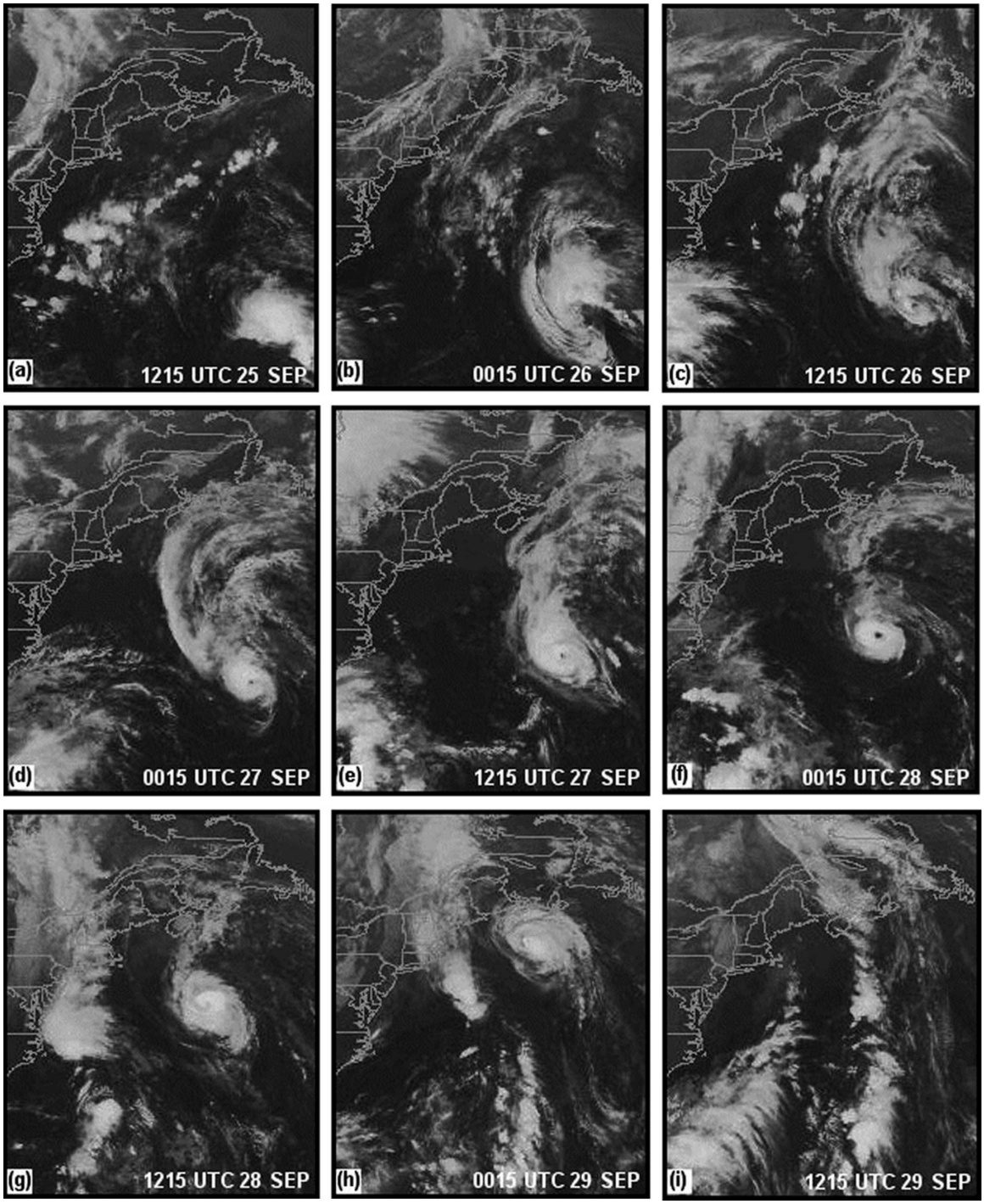

FIG. 1. GOES infrared satellite imagery showing the evolution of Hurricane Juan.

mated maximum sustained winds of 44 m s^{-1} (85 kt) and a minimum pressure of 973 hPa. Juan moved quickly across Nova Scotia and struck Prince Edward Island as a marginal category-1 hurricane, then moved into the Gulf of St. Lawrence as a strong tropical storm. The remnants of Juan moved into Labrador, Nova Scotia, during the afternoon of 29 September and dissipated as an extratropical depression. A map indicating various points of reference in the text appears in Fig. 3.

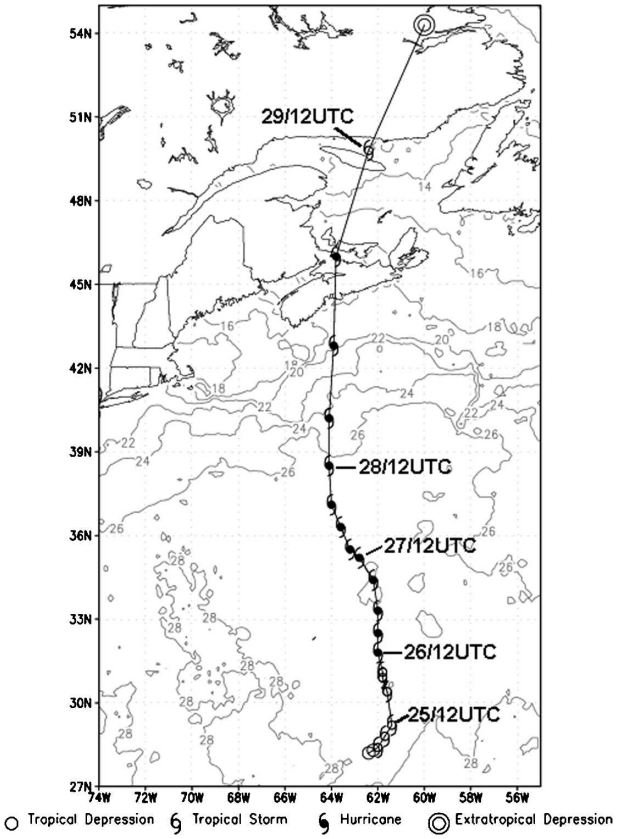

FIG. 2. Storm track (BT) for Hurricane Juan with prestorm SSTs (°C).

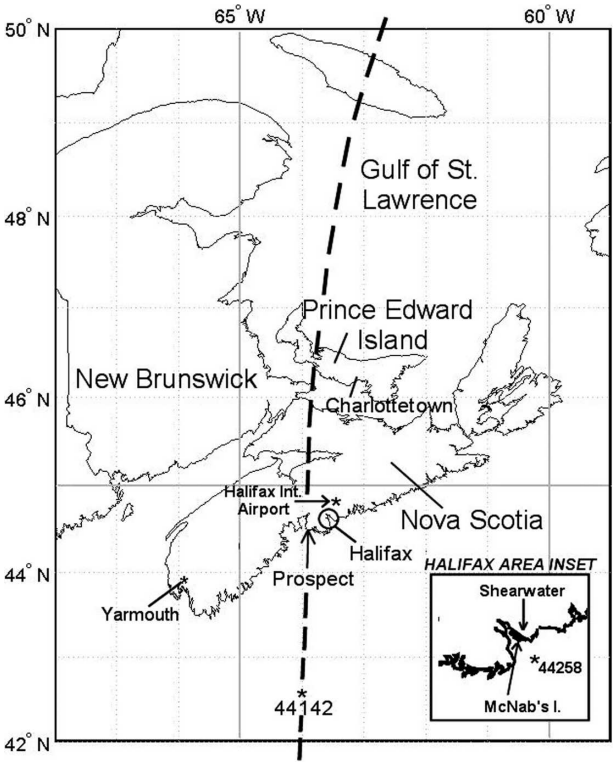

FIG. 3. Reference map for locations cited in the text.

3. Description of the modeling system

a. The mesoscale atmospheric model

The Mesoscale Compressible Community (MC2) model, version 4.9.6, is used to conduct experiments simulating Hurricane Juan using a synthetic TC vortex insertion in the initial conditions. For a general overview of the model see Benoit et al. (1997). This nonhydrostatic, fully compressible limited-area model employs three-dimensional semi-Lagrangian advection and semi-implicit time discretization to solve the primitive Euler equations on terrain-following height coordinates (Gal-Chen and Somerville 1975). The Canadian Meteorological Centre (CMC) Physics Library, version 4.0, is used for the parameterization of physical processes. A kinetic energy closure scheme described by Benoit et al. (1989) is employed in the boundary layer to parameterize turbulent transports. Monin–Obukhov similarity theory is used in the atmospheric surface layer to determine the vertical profile of the wind field and sea surface fluxes.

Grid configurations and model integration periods are shown in Fig. 4. The model is piloted by regional analyses every 6 h from the CMC Data Assimilation System archive (Chouinard et al. 1994) on a 28-km (0.25°) latitude–longitude grid covering eastern North America and the western Atlantic Ocean (20.0°–70.0°N, 100.0°–30.0°W). Two integrations of the model are conducted, one on a coarse 12-km (0.108°) latitude–longitude grid centered on the area of interest (Nova Scotia) from 30.4° to 59.6°N and from 78.2° to 45.8°W with 25 computational levels (7 in the BL), and another on a finer 3-km (0.027°) grid oriented along the storm track from 35.2° to 47.4°N and from 67.0° to 61.0°W with 40 computational levels (12 in the BL). The lowest computational level in the 3-km version is 40 m. A time step of 120 s is used in the 12-km simulations and 30 s for the 3-km simulations. For the control simulations described in the next section, the Kain and Fritsch (1990) deep convective parameterization scheme is used for the 12-km runs while convection is resolved explicitly in the 3-km simulations.

b. The synthetic storm vortex

The model initial conditions are modified by inserting an observationally consistent, TC-like vortex constructed prior to running the model. The poorly ana-

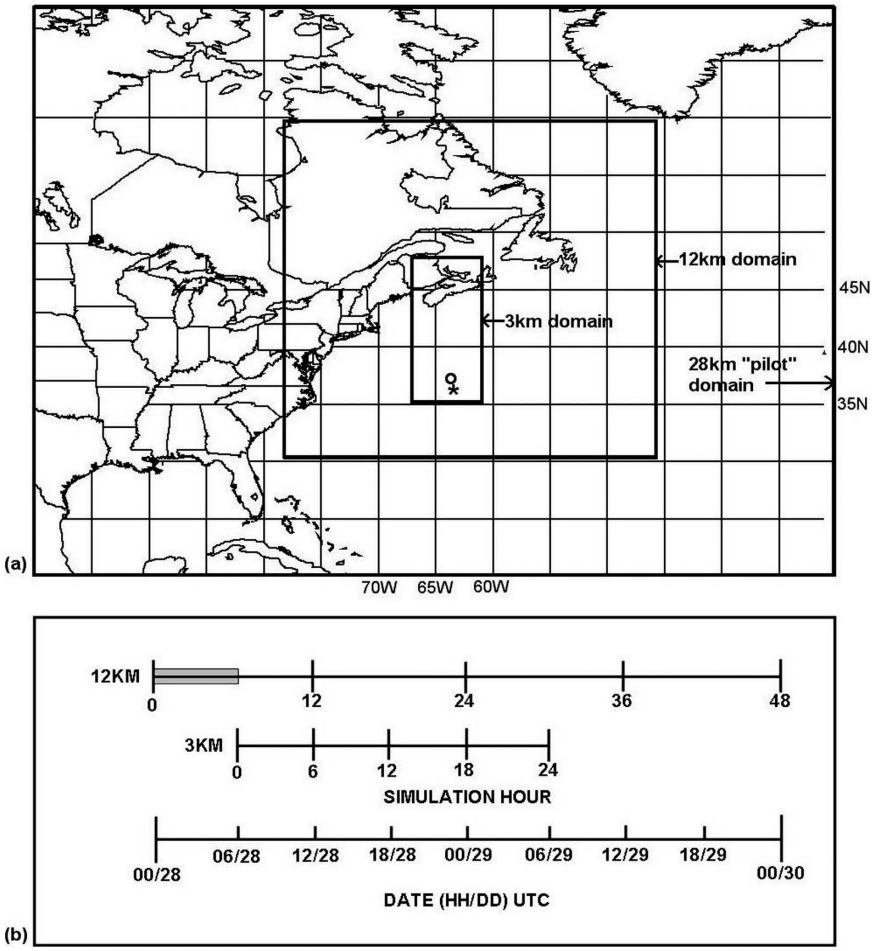

FIG. 4. Layout for the model experiments: (a) grid configuration and (b) time lines for the model integrations. The asterisk in (a) marks the storm center at time zero of the 12-km control simulations and the open circle marks the mean position of the storm at time zero of the 3-km control simulations. The gray region on the 12-km time line in (b) denotes the 6-h model adjustment period.

lyzed low in the original fields is very near the location where we insert the synthetic vortex, so the original low is completely replaced. The vortex is constructed using key observational data from the National Hurricane Center (NHC) best track (BT; Avila 2003) and from NHC operational message archives (available online at http://www.nhc.noaa.gov/archive/2003/JUAN.shtml). Control parameters for the vortex include the following: (i) the minimum central sea level pressure, (ii) storm center position, (iii) size (radius of 15 m s^{-1} surface winds, R_{15}), and (iv) the percent of the background flow used for the initial wind field asymmetry. The sea level pressure profile follows that of Fujita (1952) and is defined as a function of the radius:

$$p(r) = p_e - dp\left[1 + \left(\frac{r}{R_o}\right)^2\right]^{-1/2}, \qquad (1)$$

where $dp = p_e - p_c$ (p_e is the ambient sea level pressure and p_c is the minimum sea level pressure in the storm). R_o is the characteristic radius (smaller R_o yields a larger radial pressure gradient). For example, for a given dp, if R_{15} is decreased to give a compact storm, then R_o will also decrease. The moisture structure of the vortex is cylindrically symmetric about the storm center and defined by a moist adiabat that extends from 1000 hPa (with corresponding environmental temperature for that level) to a level where the moist adiabat intersects the environmental temperature sounding, which defines the cloud top. The relative humidity throughout the storm core is near 90% (following Davidson et al. 1993) and gradually decreases as a function of radius from the storm center. The environmental parameters (including temperature) are obtained from an annular region with inner radius of $0.6R_{15}$ and outer radius of

$2R_{15}$. This annulus is essentially the same annulus used as the blending zone for which the vortex is inserted into the environmental fields (i.e., the large-scale analysis). For a more detailed description of the synthetic vortex and the blending procedure, see Davidson et al. (1993).

The initialization procedure described above is applied at 0000 UTC 28 September to the 12-km grid. This initial time was chosen for two reasons. First, Juan was at its most developed stage (Fig. 1f), which is a desirable condition for effectively applying the synthetic vortex, and second, we are primarily interested in the spindown period of the storm over the cooler SSTs. After the 12-km simulation is completed, a second integration on the 3-km grid (using output from the 12-km grid valid at 0600 UTC 28 September) is run for 24 h. Six hours of "vortex adjustment" are required before beginning the 3-km run (see Fig. 4b). The boundary conditions for the inner domain are updated every 30 min with output from the 12-km domain, but transfer is only from the outer domain to the inner domain (i.e., one-way nesting). Note that in order to reduce the possibility of "shocking" the model, we implant the synthetic vortex into the 12-km grid instead of the 3-km grid.

4. Control simulations

The modeling system described in section 3 is used to conduct two control simulations of Hurricane Juan, one with analyzed SSTs of 28 September 2003, and the other using the monthly climatology of SSTs from Geshelin et al. (1999). Monthly mean data are used to find the equivalent climatology for 28 September using a weighted average of September and October data. The analyzed SST data have a global resolution of 37 km while the climatology data have a resolution of 18.5 km. Both SST fields are interpolated to the 28-km "piloting" domain for the model (see Fig. 4). The two control runs differ only in their SST surface boundary conditions but the SSTs are fixed in each run, that is, the model is not coupled with the ocean. A map showing the observed minus climatology SST (anomaly) over the 3-km computational domain together with the storm track is shown in Fig. 5. The preexisting SSTs were anomalously warm virtually everywhere along the storm track, with the largest anomaly of 3°–5°C, north of 41°N on the Scotian Shelf (hereafter shelf).

For fast-moving hurricanes, the storm-induced SST cooling beneath the storm center is usually small (Price 1981) so there will be little negative feedback on the storm (Emanuel et al. 2004). In a pair of test simulations on Hurricane Juan conducted by K. A. Emanuel

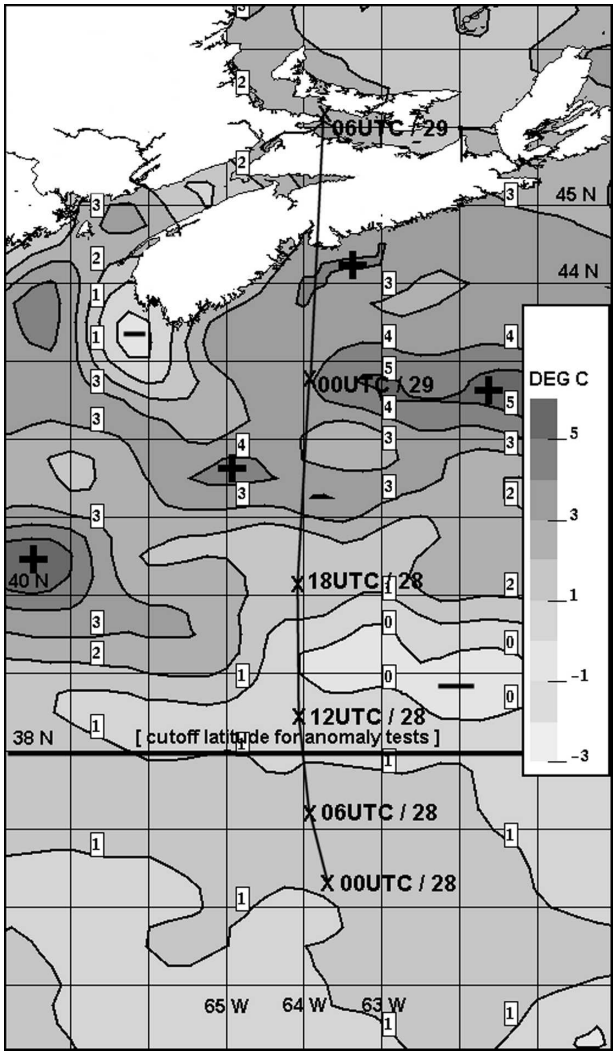

FIG. 5. Prestorm SST anomaly (°C) with storm track segment. The bold latitude line marks the cutoff for the anomaly tests. Anomaly centers are marked with plus or minus signs.

(2003, personal communication) using the Coupled Hurricane Intensity Prediction System, it was found that the storm, when coupled with the ocean, was only slightly weaker (by $\sim$1 m s^{-1} in maximum winds) than the uncoupled storm.

Figure 6 shows the tracks for the simulated hurricane in each 3-km control run where "JUAN" denotes the run with observed SST and "CLIM" denotes the run with climatology SST. Table 1 includes the vortex and model specifications for this pair of simulations. The remaining contents of the table refer to the ensemble runs to be discussed in section 5. Also plotted is the BT at 1-h increments covering the 24-h period from 0600 UTC 28 September to 0600 UTC 29 September. The simulated storm tracks follow the course of the

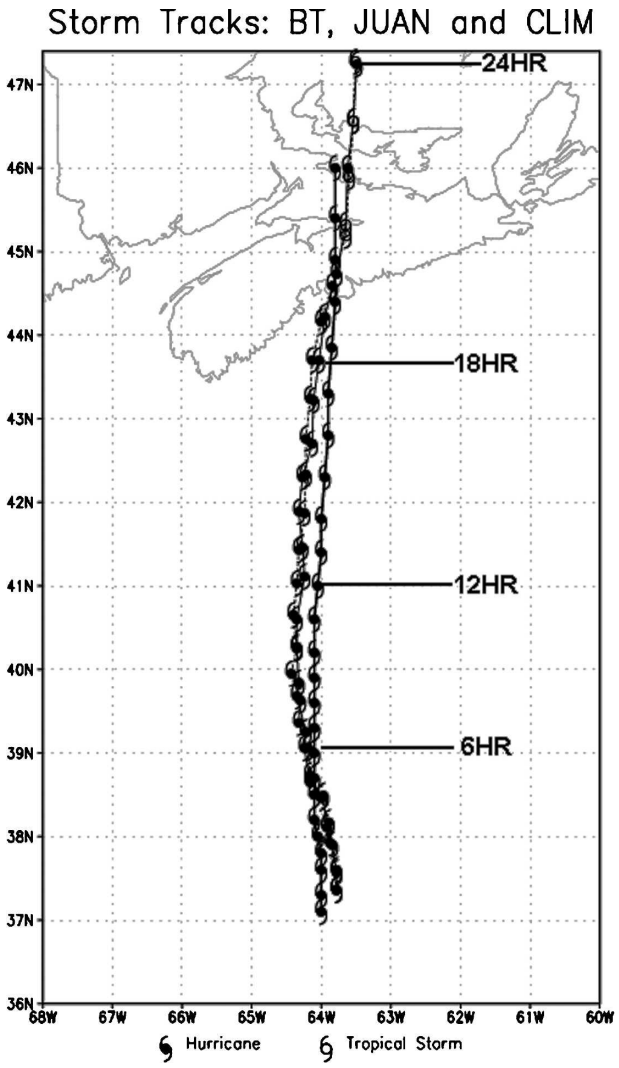

FIG. 6. Storm tracks for the JUAN (thin, solid) and CLIM (dashed) control simulations with the BT (thick, solid). Positions are marked every hour for the 24-h period from 0600 UTC 28 Sep to 0600 UTC 29 Sep. Simulation hours 6, 12, 18, and 24 are indicated and correspond to the plots in Fig. 7.

real storm rather well with two notable exceptions: 1) the simulated storms are a bit faster than reality, and 2) there is a westward jog in their tracks during the early part of the simulations. The source of these errors is yet unclear, but is consistent among the ensemble experiments that we will discuss in the next section. Much of the excess forward speed in the simulations occurs during the 6-h adjustment period, and the time in which the storm spends over the cooler waters north of the Gulf Stream is not much different than reality. Some form of assimilation cycle would be necessary to achieve optimal initial intensity and positions for the early part of the simulation. However, for the purposes of this work and as discussed by McTaggart-Cowan et al. 2006b, we feel that direct vortex insertion with a suitable (6 h) adjustment period is sufficient.

Figure 7 displays time traces of minimum sea level pressure (MSLP), maximum surface wind (MSW) speed, and SST beneath the storm center for the two control simulations on the 3-km grid and the BT. Note that the BT is not exact, that is, it is an estimate with inherent uncertainties on the order of $\sim\pm 2.5$ m s^{-1} for MSW and $\sim\pm 4$ hPa for MSLP throughout the life cycle of the storm. The CLIM storm is clearly weaker (higher MSLP) than the JUAN storm throughout the simulation on the 3-km grid. There is some difference at simulation time 0 that arises from the 6-h adjustment period on the 12-km grid, otherwise the difference in MSLP between the two runs mostly develops during the first 3 h of the simulations. There are two weakening trends later in the integrations: 1) as the storm moves over cooler shelf waters, and 2) as the storm moves over land as indicated by two different slopes in the MSLP trend curves. Note that the modeled storms make landfall sooner than the real storm as indicated by the earlier onset of rapid weakening compared with the BT. As the storm moves over the shelf waters, the MSW does not change significantly in the JUAN run but decreases steadily in the CLIM run. This behavior suggests that the wind field is becoming more decoupled from the cool marine boundary layer in the CLIM simulation. Winds from the JUAN run (Fig. 7b) more closely resemble those in the BT, although this is not exactly the case with respect to MSLP (Fig. 7a) indicating that the wind–pressure relationship in the model may not be representing reality perfectly. One final point to note here is that the increasing trend in MSW at the very end of the time series plots is artificial, since the storm is near the northern boundary ("buffer" zone) of the model domain. We are concerned with the behavior of the storm much farther south in the center of the domain.

A fictitious control run is also conducted where all SST values below 26°C are made equal to 26°. In this scenario, the hurricane has no opportunity to weaken while approaching Nova Scotia, and in fact intensifies to a category-3 hurricane (MSW of 54 m s^{-1} or 105 kt) at landfall (not shown). This indicates that the situation for Nova Scotia would have been *much worse in the absence of the storm-tempering effect of cooler shelf waters.*

Before proceeding, we wish to clarify that when referring to the best track, MSW is defined as the maximum 1-min mean (sustained) winds anywhere in the storm at 10 m above the surface. When referring to output from the model, MSW is the maximum instantaneous (e.g., snapshot) surface wind anywhere in the

TABLE 1. List of experiments used in the study. JUAN and CLIM are the control runs using observed and climatology SST, respectively. Lat and lon indicate the storm center position, basicp is the fraction of the background flow used to prescribe the initial wind field asymmetry, convec is the convective parameterization scheme (abbreviations are explained in the text), and the final column indicates the number of computational levels in the model with the number in parentheses indicating the number of levels in the BL. Changed parameters in each experiment are set boldface.

Expt	MSLP (hPa)	Lat (N)	Lon (W)	R_{15} (km)	Basicp (frac)	Convec	Computational (BL) levels (3 km)
JUAN and CLIM	970	36.3	63.6	250	0.75	kfc	40 (12)
EM1	970	36.3	63.6	250	**0.50**	kfc	40 (12)
EM2	970	36.3	63.6	250	**1.00**	kfc	40 (12)
ES1	970	36.3	63.6	**225**	0.75	kfc	40 (12)
ES2	970	36.3	63.6	**300**	0.75	kfc	40 (12)
ES3	970	36.3	63.6	**350**	0.75	kfc	40 (12)
EI1	**966**	36.3	63.6	250	0.75	kfc	40 (12)
EI2	**974**	36.3	63.6	250	0.75	kfc	40 (12)
EP1	970	36.3	**64.0**	250	0.75	kfc	40 (12)
EP2	970	**36.6**	63.6	250	0.75	kfc	40 (12)
EP3	970	36.3	**63.2**	250	0.75	kfc	40 (12)
EP4	970	**36.0**	63.6	250	0.75	kfc	40 (12)
EC1	970	36.3	63.6	250	0.75	**fcp**	40 (12)
EC2	970	36.3	63.6	250	0.75	**kuo**	40 (12)
ER1	970	36.3	63.6	250	0.75	kfc	**32 (9)**
ER2	970	36.3	63.6	250	0.75	kfc	**48 (15)**

storm, where surface is defined at the 40-m (lowest computational) level. We find that the 40-m winds from the model are a more reasonable representation of reality than the 10-m diagnostic winds from the model. We will elaborate on this in section 4b.

a. Comparison with aircraft data

The Canadian National Research Council's Convair-580 aircraft conducted a mission into Hurricane Juan just prior to landfall. Meteorological data from 25 GPS dropsondes were collected, and we use the data here to compare with output from the model. Southwest–northeast cross sections of wind speed and equivalent potential temperature parallel to the Nova Scotia coastline are shown in Fig. 8, along with corresponding views from the model. A more detailed description of the aircraft and equipment is given by Abraham et al. (2004).

The wind field in Hurricane Juan was very asymmetric with much stronger winds occurring over a deep layer of the troposphere on the east side of the storm, probably because of the rapid forward translation speed of $\sim$15 m s^{-1}. This structure is apparent in Figs. 8a,b. The center of the storm in these images is near dropsondes 16 and 17 where the gradient in wind speed drops off dramatically. No wind data were collected in certain parts of the storm since there were problems with GPS receiver reception. These are the blank areas in Fig. 8b. The model helps us to fill in these holes in the observational data. Aside from the data void, the structure of the wind fields compares rather well especially with regard to the thickness of the layer of strong winds and the wind shear in the BL.

The warm core of Juan just prior to landfall is depicted in Figs. 8c,d with cross sections of equivalent potential temperature θ_e calculated using the formulation of Bolton (1980). Overall, the air mass in the model is warmer/moister than the observations indicate, yet the model captures the main features. In particular, there is a narrow strip of high θ_e in the storm core with values of 345 K and higher. There is also a region of lower θ_e air that is collocated with the region of strongest winds that suggests that the storm was mixing with cooler/drier environmental air and from contact with the cooler ocean surface. We also see a slight tilt in the warm core with height that is detected in the model as well.

A cross section of θ_e taken from the CLIM simulation is shown in Fig. 8e. This is the same view as the panels discussed above. There is a remarkable difference in low-level θ_e beneath the storm core when comparing JUAN (Fig. 8c) and CLIM (Fig. 8e). It appears that a cold θ_e dome has formed below $\sim$850 hPa at the circulation center of the CLIM storm, suggesting *thermodynamic decoupling* of the warm core from the sea surface. This dome does not appear to be present in the JUAN simulation. It is interesting, but not surprising, that the CLIM storm was rapidly weakening (with respect to MSW) at this time, while the intensity of JUAN was almost steady (see Fig. 7b).

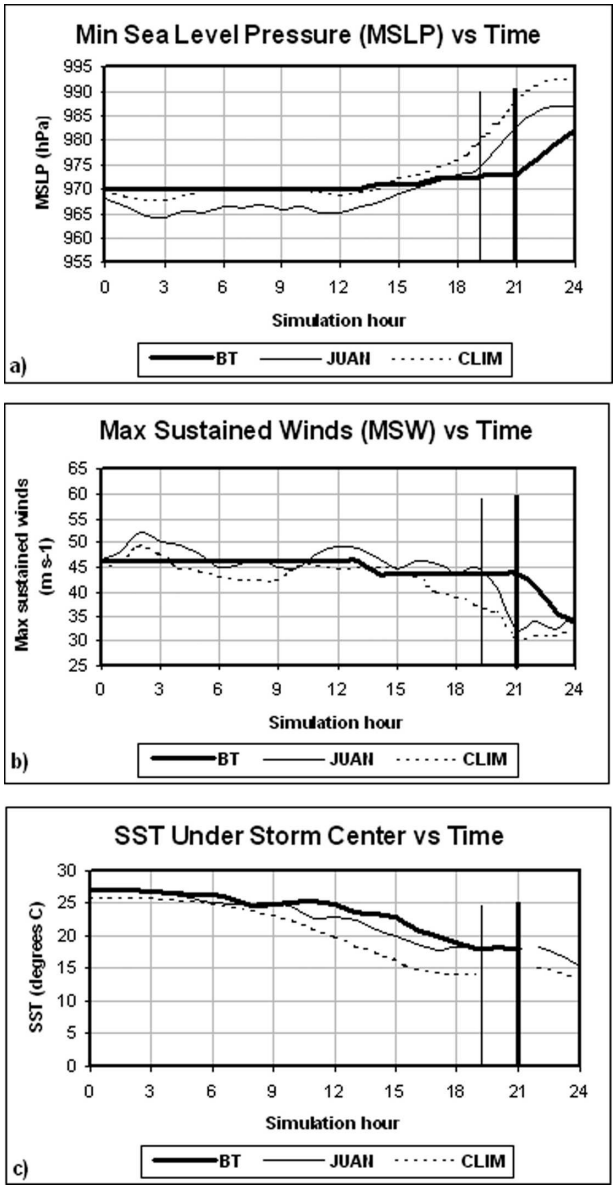

FIG. 7. Model results for the control simulations: (a) evolution of MSLP for JUAN (thin, solid), CLIM (dashed), and the BT (thick, solid); (b) MSW; and (c) SST beneath the storm center as a function of model simulation time (hours). Vertical lines indicate time of landfall for the simulations (thin) and BT (thick).

b. Comparison with surface data

Figure 9 shows contours of sea level pressure and isotachs of 40-m winds from the JUAN and CLIM simulations, plus an analysis of sea level pressure obtained from various surface observations. The central pressure of 973 hPa in Fig. 9a was estimated from dropsonde surface data just prior to landfall. The valid times are 0100 UTC 29 September (19 h into the simulation) for the model output and 0300 UTC 29 September for the analysis. These staggered times are chosen for spatial comparison because the modeled storm makes landfall ~1.5 h earlier than reality. This corresponds to a track error of 110 km. As a matter of comparison, the NHC operational track forecast error (based on several numerical models) for the 24-h period ending 0000 UTC 29 September was 170 km (too far north), while our simulated track error is 100 km for the same period. Many of the operational numerical models had a fast bias with this storm, including the official forecasts. As noted earlier in this section, most of the positional error in our simulations occurs during the 6-h adjustment period. The storm speed after that period is modeled very well. Aside from the early arrival time, the storm structure at landfall in the JUAN run (Fig. 9b) compares well with the analysis (Fig. 9a). The model quite accurately pinpoints the landfall location, intensity (44.8 $m\,s^{-1}$ versus the best track of 43.8 $m\,s^{-1}$) and the radius of maximum winds (~45 km versus the observed ~35 km) approaching the metro Halifax area of Nova Scotia. The CLIM run generates a weaker storm just prior to landfall (Fig. 9c) with maximum surface winds ~7.3 $m\,s^{-1}$ weaker (37.5 $m\,s^{-1}$) than the JUAN run (i.e., category-1 versus category-2 hurricane). The track is virtually unaffected by the difference in SST in this pair of control runs, and the same is true of the ensemble experiments to be discussed in section 5.

We also wish to investigate the surface winds as a function of time for various weather stations, and compare them with the model results. Four points are chosen for analysis, they are: Halifax International Airport (an inland station), Shearwater (a coastal station), McNab's Island (an exposed island station), and Buoy 44142 (well away from the coast). Locations of these sites are shown in Fig. 3. The data and model results are plotted in Fig. 10. Note that model (instantaneous) surface winds are valid at 40 m (lowest computational level) and stations are valid at 10 m.

There is a clear temporal separation between peak winds from the model compared with these sites owing to the faster-simulated storm. Putting this difference aside, we focus on comparing the peak winds from the model with data. At Halifax International Airport (Fig. 10a) the maximum surface winds from the model were ~24 $m\,s^{-1}$, which is an underestimate compared with the observed winds (~28 $m\,s^{-1}$). The difference between JUAN and CLIM winds is greatest at the airport site. In fact, if we work out the maximum wind power per unit area which is given by $\frac{1}{2}\rho U^3$, where U is the 10-m sustained wind speed and ρ the density of air, we see that the winds in the JUAN run are approximately 2 times more powerful (i.e., more destructive) than the CLIM run. At the Shearwater site (Fig. 10a) the model

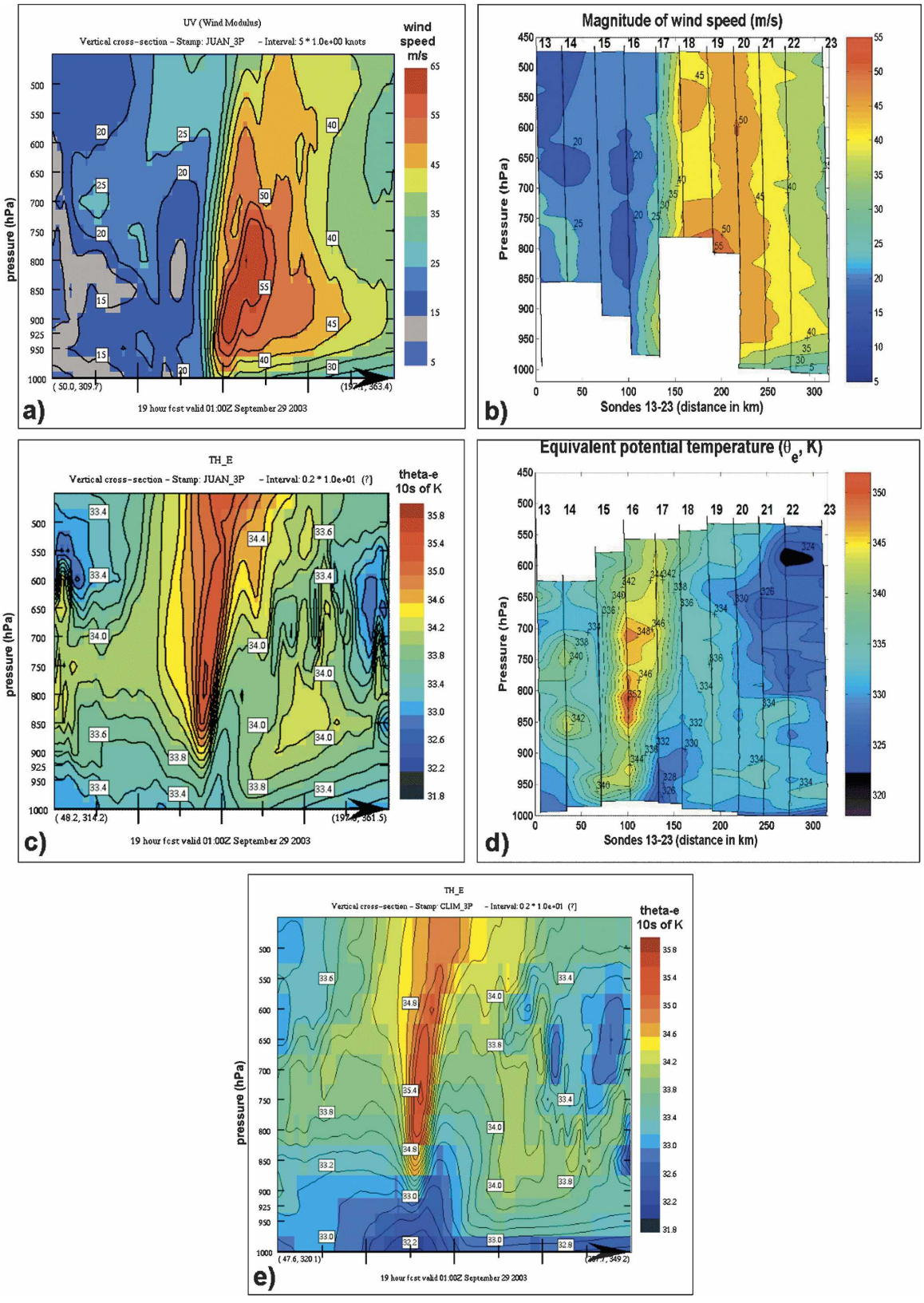

FIG. 8. Vertical cross sections of wind speed and θ_e near landfall. (a) Output of wind speed (m s^{-1}; every 5 m s^{-1}) from the JUAN control run as a function of pressure and distance compared with (b) dropsonde data. The horizontal scale in (a) is the same as (b). Output of θ_e (K; every 2 K) from the (c) JUAN control run and (e) CLIM control run compared with (d) dropsonde data. The location of dropsondes in (b) and (d) are shown by vertical lines and are numbered.

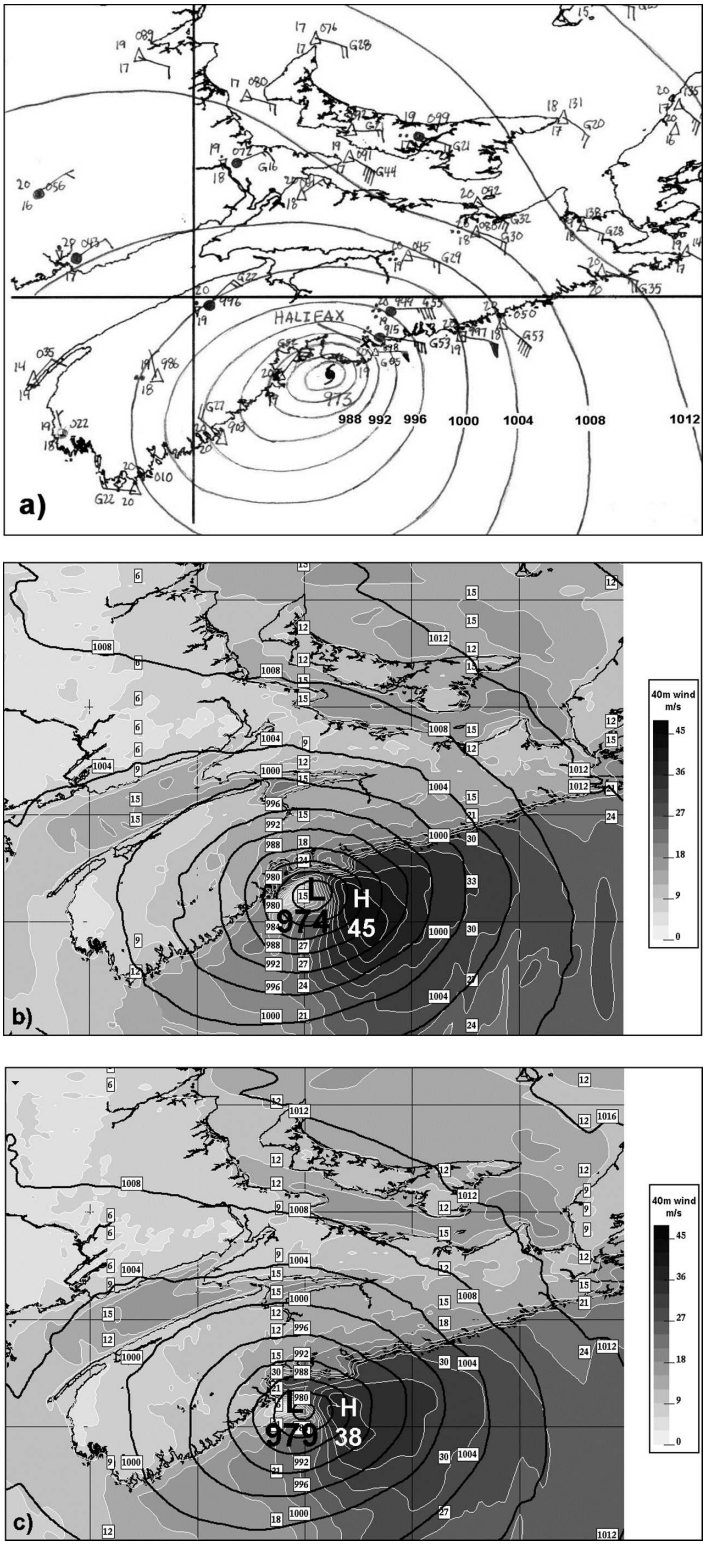

FIG. 9. Hurricane Juan just prior to landfall: (a) hand-drawn analysis of SLP (solid contours every 4 hPa) with weather station data plotted using conventional synoptic format; output from the (b) JUAN control and (c) CLIM control simulations showing SLP (black contours) with 40-m wind speed (shaded field every 3 m s^{-1}).

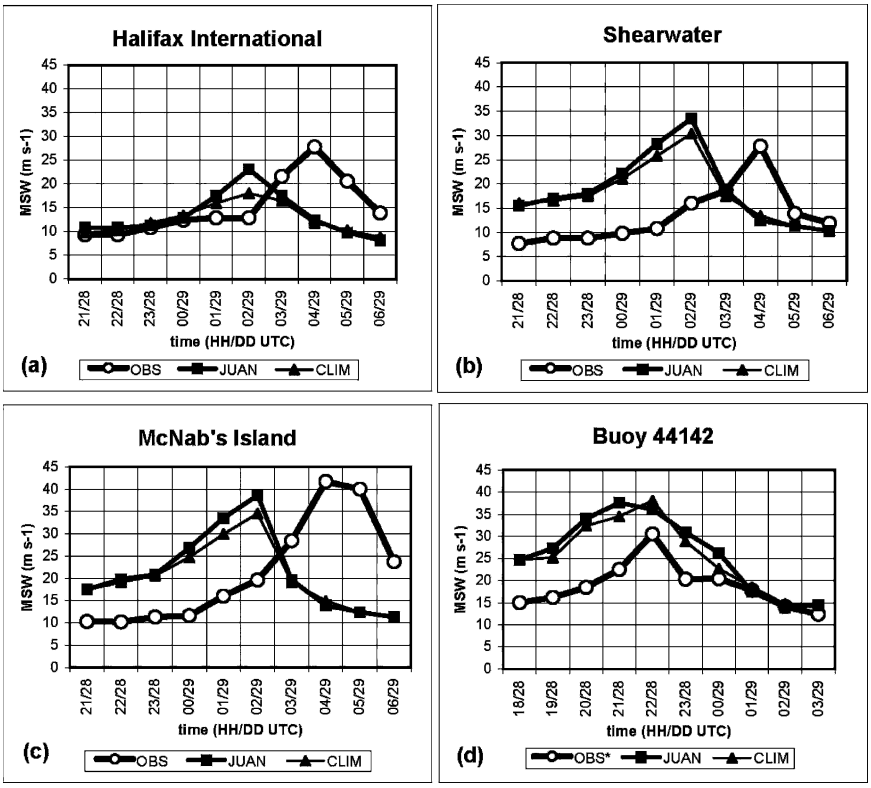

FIG. 10. Time series output of instantaneous surface wind speed from the model (valid at 40 m) and from weather stations (valid at 10 m) for various locations: (a) Halifax International Airport, (b) Shearwater, (c) McNab's Island (Halifax Harbour), and (d) buoy 44142 (~200 km south of storm landfall location).

overestimates the winds. At the exposed McNab's Island station (Fig. 10c) the model underestimates the winds by a small amount (3.1 m s^{-1}). This site reported the highest wind speeds of any station at landfall and was important in rendering Juan as a category-2 hurricane at landfall. At this site, the maximum winds from the CLIM simulation work out to be ~70% as destructive as the winds in the JUAN run.

Juan moved almost directly over buoy 44142, yet the maximum winds observed at the buoy were only around 30 m s^{-1} (Fig. 10d). This is likely a result of the coarse sampling period of 1 h (missing the peak winds), and the fact that the anemometer is only 5 m above the water and may have been sheltered in the high seas. The corrected standard 10-m observed winds are shown in Fig. 10d using a logarithmic profile described in Shearman (1989) and given by

$$U(z) = \frac{u_*}{k} \ln \frac{z}{z_o}, \tag{2}$$

where $U(z)$ is the wind speed at height z, u_* is the friction velocity, k is the von Kármán constant ($k = 0.4$), and z_o is the roughness length in meters ($z_o = 0.0016$ is a typical value over water).

These results indicate that there is considerable point-to-point variability in the model's representation of wind speed. However, the 40-m model winds are generally more representative of observed winds than are the 10-m diagnostic winds from the model (not shown), especially over land. A microscale model of the BL would likely be necessary to capture the details of the wind field at the 10-m level

Unlike most hurricanes, Juan did not produce a significant amount of precipitation, owing to its rapid forward speed of motion and the loss of convection on the south side of the storm. The model does a very good job replicating the northward-skewed rainfall pattern and the aerial distribution of rainfall. On the other hand, rainfall amounts are overestimated as shown in Fig. 11 when compared with rain gauge data (Fig. 11a). For example, at Shearwater there were only 25 mm of rain while the model generated approximately 50 mm. The moisture content in the simulated storm seems to be overestimated as indicted by the high values of equivalent potential temperature in Fig. 8 compared with ob-

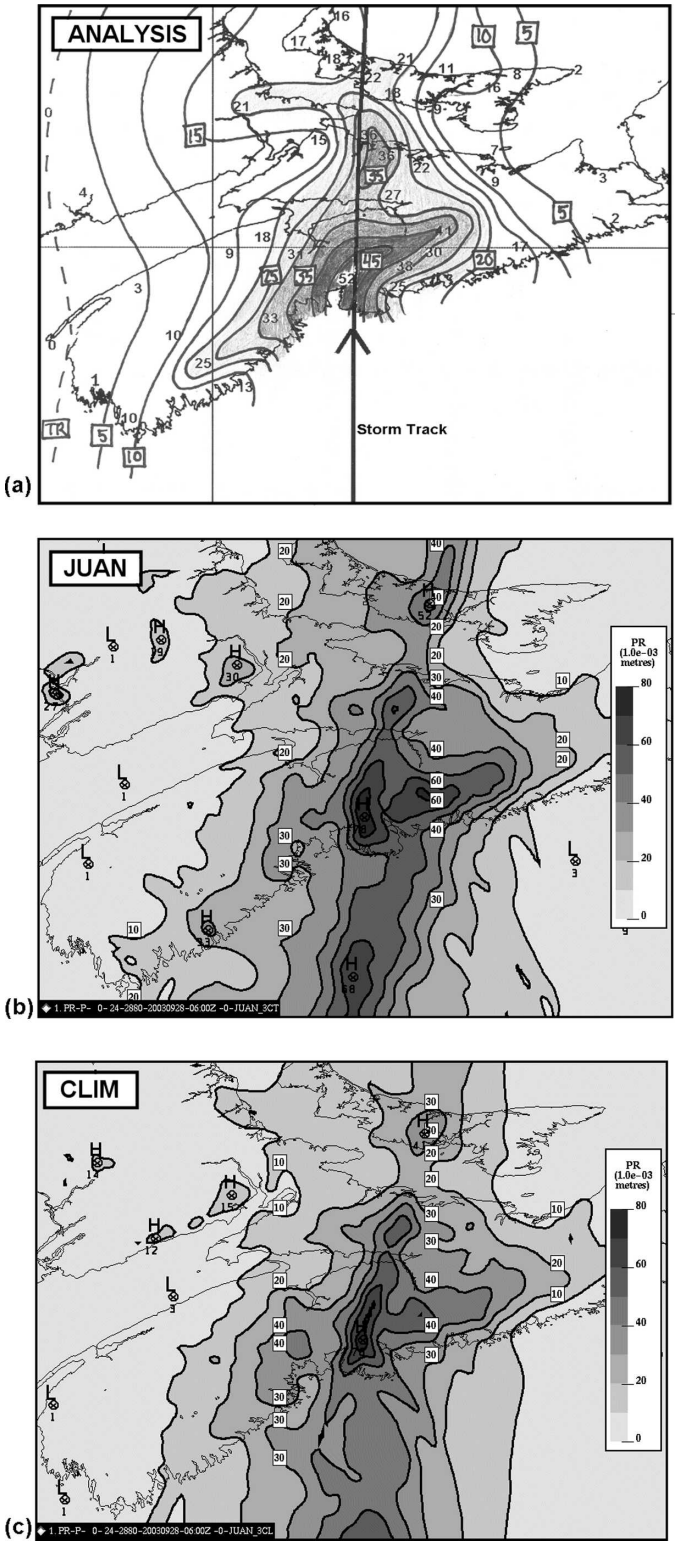

FIG. 11. Storm total rainfall accumulations: (a) subjective analysis (solid contours every 5 mm) with various station amounts indicated by individual numbers; model-generated rainfall from the (b) JUAN control and (c) CLIM simulations (shaded contours every 10 mm).

servations. It is therefore reasonable to expect such an air mass would generate greater rainfall. Model-simulated rainfall from the CLIM run (Fig. 11c) is somewhat less than the JUAN run. The difference is approximately 10 mm near the maximum rainfall region.

c. Vertical wind profiles

Snapshots of vertical profiles of wind speed from the model simulations are shown in Fig. 12 for two selected locations: one over the ocean within the high wind region and the other over land. The overwater profiles (Fig. 12a) were chosen at the location of the strongest surface winds in each storm (JUAN and CLIM) just prior to landfall. The height and strength of the low-level jet over the ocean in the CLIM run clearly differs from the JUAN run. The CLIM jet is ~150 m lower (~350 m versus ~500 m) and the magnitude is ~12 m s^{-1} weaker based on these model output levels. The lower jet height suggests a shallower atmospheric BL over the cooler ocean in CLIM, consistent with greater boundary layer stability (Stull 1988). Well away from the high wind region, we observe the jet heights in both cases to be on the order of 1000 m, which is much higher than in the storm core region (not shown). This is typical in hurricanes and is described by Franklin et al. (2003). The overland profiles (Fig. 12b) were extracted at Halifax International Airport at the time when model winds were strongest there. The jet height is much higher (~1000 m) than in the vicinity of the maximum wind over water.

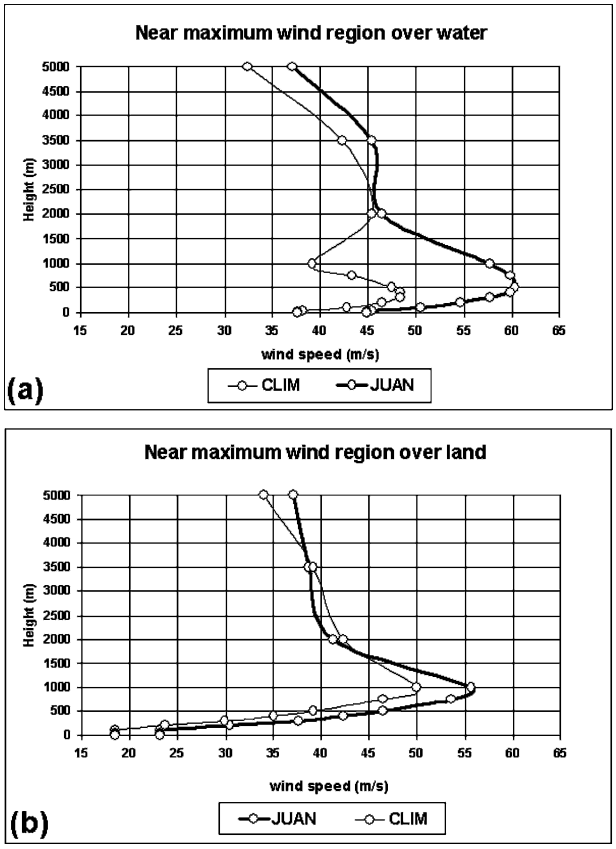

FIG. 12. Vertical profiles of wind speed from the model for (a) the high wind region in the storm over water just before landfall, and (b) the high wind region at Halifax International Airport (when winds were strongest there) from the JUAN (solid, bold curve) and CLIM (solid, thin curve) simulations.

5. Model ensembles

a. Description of ensemble experiments

To provide a stronger argument for the role of anomalously warm SSTs on the weakening rate of Hurricane Juan, 15 additional simulations were conducted for each of the two SST configurations (JUAN and CLIM), giving a total of 30 additional experiments. Most of the ensemble members involve perturbation of the vortex parameters (initial conditions) such as storm position, size, and intensity (central pressure) within their observational error bounds. This serves as an effective way to gauge the sensitivity of the simulations to the initial conditions as well as other factors associated with the model itself, in particular, convective schemes and vertical resolution of computational levels. A summary of the ensemble experiments is shown in Table 1.

One of the vortex parameters that can be tuned is the percentage of the background flow used as a proxy for the wind field asymmetry and maximum surface winds in the initial specified vortex for a given MSLP. The default value is 75%, but we run two ensemble members whereby the value is changed to 50% and 100%. The corresponding initial maximum surface wind speeds for 50%, 75% and 100% are 44, 47, and 51 m s^{-1}, respectively. These values are similar to the range of error for winds in the best track, namely ±2.5 m s^{-1}. Choosing 75% yields a value closest to the best track (46 m s^{-1}) valid at 0000 UTC 28 September.

The second set of ensemble members involves adjustment of the initial vortex size R_{15}. The storm track and intensity is far more sensitive to this than to any of the other parameters. In the control experiments we use 250 km, which was determined from the mean gale radius included in the NHC bulletin archive (available online at http://www.nhc.noaa.gov/archive/2003/JUAN.shtml?). A suitable scaling was determined for

adjusting the radius of gales (17.5 m s^{-1}) to R_{15} using Eq. (1), noting that for gradient balance

$$\frac{U^2}{r} + fU = \frac{1}{\rho}\frac{\partial P}{\partial r} \tag{3}$$

and solving for radius r in terms of wind speed U.

An additional pair of ensembles consists of adjusting the initial storm intensity, which is done via perturbation of the MSLP. At 0000 UTC 28 September (the start time of the model) the MSLP of Juan was estimated to be 970 hPa, but the error in that value is approximately ±4 hPa, so we use that as a basis for the ensemble pair (966 and 974 hPa). Four more members are generated by perturbing the initial storm location by 37 km (approximately three grid points) in each cardinal direction. The advertised positional error for Juan at 0000 UTC 28 September was 37 km (20 nm) based on information from the NHC bulletin archive.

Four additional members are created by adjusting the convective scheme of the 12-km run of the model and by changing the number of vertical computational levels on the 3-km grid. The convective scheme in most runs is given by Kain and Fritsch (1990) while two of the members use the Fritsch and Chappel (1980) and Kuo (1974) parameterizations. The default number of computational levels is 40 (top level at 35 000 m), with 12 levels in the BL (below 1500 m). There are 32 (9) levels in one member and 48 (15) in the other member, where the number of BL levels is in parentheses.

Our main objective for running an ensemble of experiments is to determine whether the difference in intensities between the control simulations (JUAN and CLIM) is statistically significant. Before presenting the collective results from the ensembles, we wish to briefly discuss the highlights from some of the ensemble sets discussed above. Please refer to Table 1 for the list of experiments.

b. Overview of model sensitivities

By increasing the storm's initial wind field asymmetry, the storm drifts farther to the west during the first 12 h of the simulation (experiment EM2) while the storm whose initial wind field asymmetry is weakest (EM1), moves more slowly during this period and does not drift to the west. It is possible that there is something in the storm environment that is causing the storm to track farther to the west, and that the more asymmetric and faster-moving storm (EM2) is encountering the feature sooner.

The simulated storm intensity appears to be most sensitive to initial storm size. The smallest storm (R_{15} = 225 km) weakens prematurely while the largest storm (R_{15} = 350 km) does not weaken fast enough with central pressure remaining just above 970 hPa after landfall. The control storm size (R_{15} = 250 km) yields the best landfall intensity with respect to central pressure. It is no surprise that the larger storms weaken at a slower rate because it takes longer to spin down a large vortex versus a smaller one. It is also observed that the larger storms take a more easterly track across Nova Scotia after landfall. The smallest storm stays farthest to the west of any ensemble member. It is likely that the larger storm interacts differently with the (steering) environment than the smaller storm.

Investigation of the impact of initial storm intensity on the simulation shows that the simulation starting with central pressure of 974 hPa yields a more realistic trend in SLP and MSW compared with the BT and even compared with the control runs with an initial pressure of 970 hPa. When starting with a central pressure of 966 hPa, the model deepens the storm too much initially and then weakens it too rapidly. The SSTs are likely not warm enough to support this intense storm and the consequence is an unrealistic weakening trend.

The greatest impact of adjusting the initial storm position was on the storm track. The run with initial position farthest to the north yielded the greatest westward deviation in track and earliest landfall time (by just over 2 h). A noticeable westward deviation was also observed in the initially more asymmetric and faster-moving member (EM2), which supports the claim that there was likely something in the environment ahead of Juan that may have induced the westward jog in the track in those simulations.

Although convection is explicitly computed on the 3-km grid, we detect impacts on the storm track and intensity when using different convective schemes in the 12-km "driving" grid (refer to Fig. 4b for model integration layout). These 12-km simulations provide the initial and boundary conditions for the corresponding 3-km runs, which ultimately lead to somewhat different solutions. One key observation using the Fritsch–Chappel (FCP) and Kuo (KUO) schemes is that the MSLP slowly rises during the early part (first 6 h, i.e., the adjustment period) of the 12-km simulations while in the Kain–Fritsch (KFC) (control) simulations the MSLP slowly falls during this period. The trend in MSLP during the first 6 h of the 3-km simulations driven by the 12-km simulations that use FCP and KUO convection is much steadier than for KFC convection. The KUO member actually yields a better result than our control run (JUAN). The track is very good (aside from the speed), and the MSLP and MSW are close to the BT curve (not shown). When run with

the observed SST, this member shows that the MSW speeds are actually increasing slightly as the storm makes landfall (possibly the storm acceleration affect), while the climatology SST run of that member shows decreasing winds during the prelandfall hours.

The final set of ensemble members are generated by altering the vertical resolution of the model. By increasing the number of levels throughout the troposphere and in the BL, the intensity of the storm is closer to the BT, especially while the storm is approaching land. The runs with coarser vertical resolution seem to lead to an overestimation of storm intensity. With fewer levels in the BL, the estimation of surface (40 m) winds tends to be biased on the high side because winds are computed at a higher level (with stronger winds) than in the member with finer vertical resolution.

c. Analysis of ensemble means

A composite map showing the tracks of all 15 ensemble members from the observed SST (JUAN group) including the control run and the best track is shown in Fig. 13. The members are rather well clustered with no extreme outliers. The along-coast spread in landfall positions is ~100 km. The westward drift in the tracks during the early part of the simulations is apparent in the composite. The *maximum* positional error at the end of the 24-h simulations was ~160 km, which compares to the *mean* 24-h operational NHC forecast error of ~150 km for this event (see Avila 2003).

Figure 14 shows time series of ensemble means of MSLP and MSW for each group of members (JUAN and CLIM) including the control runs (16 runs compose each curve). There is a consistent difference between the intensity of the JUAN members compared with the CLIM members. In terms of MSW, the difference is smallest near the beginning of the simulations and is greatest at 19 h, which represents the landfall time of most members. The actual difference in landfall intensity works out to 4.9 m s^{-1} with a standard deviation of 1.6 m s^{-1}. This difference is statistically significant at least at the 99% confidence level using a paired *t* test. Even the difference at hour zero is significant at the 99% confidence level. An important observation here is that the mean rate of prelandfall weakening (in terms of MSW) in the CLIM members is greater than the JUAN members during the hour leading up to landfall. Also, we note that there is a period of strengthening in the winds between 7 and 13 h in both cases corresponding to a period when the storm is already moving over cooler water. It is likely that this is related to acceleration of the storm during that time.

It is clear from the results that a sizable fraction of the difference (3.1 m s^{-1}) between simulated storm intensities for each ensemble group (i.e., the JUAN and CLIM group) occurs by 4 h into the model run. In fact, the difference between the groups begins during the 6-h, 12-km adjustment period, since at 0 h there is already a difference in intensities (1.4 m s^{-1}; see Fig. 4b for time reference). Between 4 and 18 h there is little change in the spread between the groups, and it is not until the 1- to 2-h period prior to landfall that the spread increases to 4.9 m s^{-1} (e.g., the intensity of the JUAN group levels off while the CLIM group continues to rapidly weaken). In other words, ~65% of the difference in intensities between the two ensemble groups occurs during the early part of the simulation when the storm was over a weak warm anomaly of

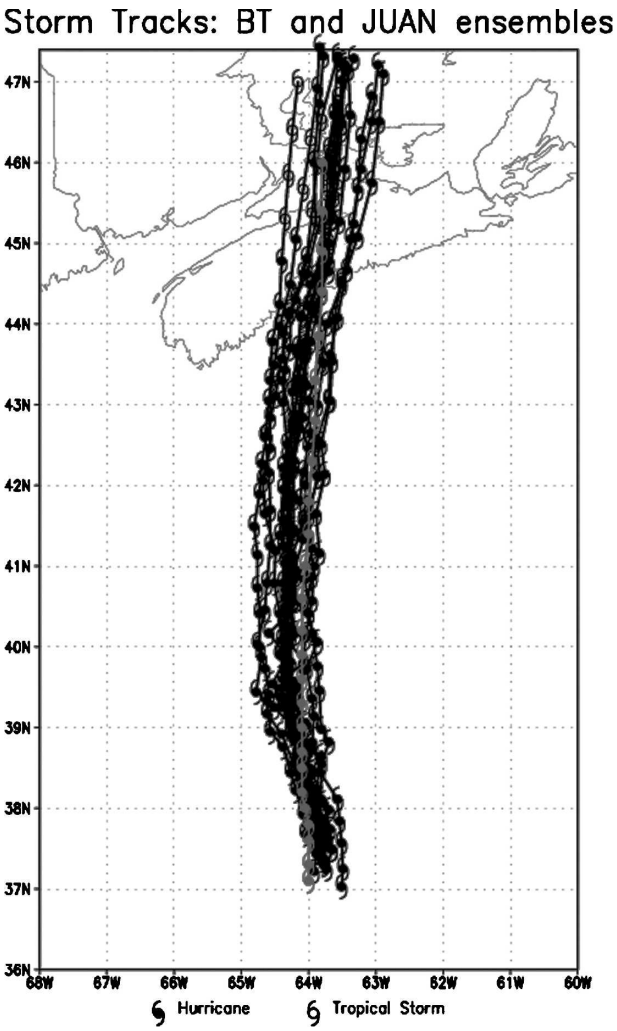

FIG. 13. Storm tracks of all ensemble members (including control) from the JUAN set of simulations (black), including the BT (gray). Track positions are every hour for the 24-h period from 0600 UTC 28 Sep to 0600 UTC 29 Sep.

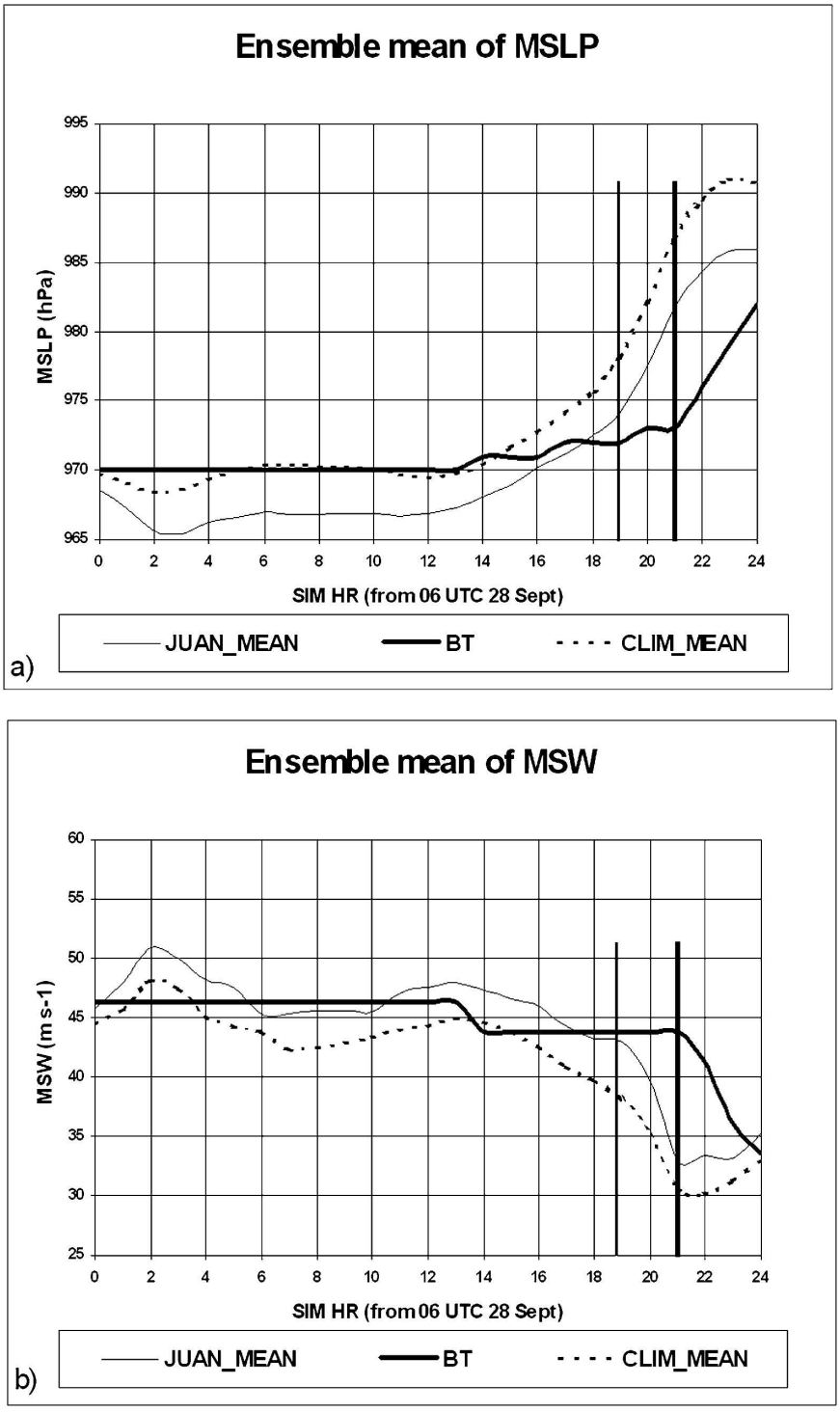

FIG. 14. Time traces of 15-member (plus control) ensemble means for the JUAN and CLIM groups of simulations: (a) MSLP and (b) MSW. Mean time of simulated landfall is shown by the thin vertical lines and the time of BT landfall is shown by the thick vertical lines.

1°–1.5°C south of ~38°N (see Fig. 5). This would lead one to suspect that a significant contribution to storm intensity at landfall is owing to this weak warm anomaly, and that the shelf anomaly (between ~41°N and the Nova Scotia coast) has a secondary contribution. In section 5d we separate the impact of these SST anomalies on landfall intensity.

d. Role of specific SST anomalies

There appear to be two zones of anomalously warm SST influencing the intensity of Hurricane Juan in our simulations. Referring to Fig. 5, there is a 1°–1.5°C warm anomaly south of 38°N over which the storm tracked. Between 38° and 39.5°N the SST is near normal, while it is well above normal north of 41°N.

To diagnose the roles of these anomalies individually, we run groups of simulations for two SST configurations, one with the SST anomaly south of 38°N removed (group S38) and the other with only the northern (shelf) anomaly removed (group N38). These groups of reruns are based on a subset of the 15-member ensemble discussed earlier. Specifically, they include one member from each of the following experiments (see Table 1): EM1, ES2, EI2, EP2, EC2, and ER2. This selection of experiments is based on members demonstrating the greatest overall sensitivity (in terms of maximum surface wind speeds at landfall) to SST from the original set of simulations. This increases the likelihood of being able to distinguish the role of the individual anomalies.

The results from these experiments are plotted in Fig. 15 together with a subset of ensemble means (see section 5c) corresponding to the experiments listed above. It is clear that the near-landfall intensity is primarily dependent on the SST anomaly on the shelf. For example, by removing the shelf anomaly (N38), the near-landfall intensity is the same as climatology (Fig. 15b). To test the hypothesis that the near-landfall intensity of the N38 ensemble subset *differs* from climatology we use a paired t test on the 18-h MSWs and compute a t value of 0.5 with 6 degrees of freedom. With this very small t value we can certainly reject the alternative hypothesis that the means are different and conclude they are equal. Conversely, when we remove the southern anomaly (S38) and test whether this ensemble *differs* from the JUAN ensemble, we find a t value of 0.4 and draw a similar conclusion. We see that by removing the shelf anomaly the storm responds rather quickly to the ocean beneath it and the intensity (as measured by MSLP and MSW) switches from an "anomalous" state to a "climatological" state over a 6–8-h period. The converse is also true.

6. Summary and conclusions

A mesoscale atmospheric model with synthetic storm vortex insertion was used to conduct experiments simulating Hurricane Juan's approach to Nova Scotia, Canada, in September 2003. Insertion and merging of the synthetic hurricane vortex into the initial large-scale analysis drastically improves the model's simulation of the storm (cf. operational weather models that did not employ vortex insertion), as discussed in detail by McTaggart-Cowan et al. (2006b). The model system was used to study the role of anomalously warm SSTs on the intensity of Juan on its approach to Nova Scotia, and to study the sensitivity of storm track and intensity to various parameters using an ensemble of model configurations and initializations.

The primary result of the work revealed that there was a statistically significant impact of the anomalously warm SST south of Nova Scotia on the simulated intensity of Hurricane Juan. The mean landfall intensity of the simulations using observed SST (JUAN), as measured from the maximum surface winds, was 42.5 m s^{-1} compared with 37.6 m s^{-1} for the simulations with climatology SSTs (CLIM). The difference was 4.9 m s^{-1} with a standard deviation of $\pm$1.6 m s^{-1}, and is significantly different from 0 at the 99% confidence level. Since the destructiveness of wind is proportional to the power of the wind (which is proportional to wind speed cubed), the CLIM storm was only ~70% as destructive as the JUAN storm at landfall.

Simulations proved very sensitive to a number of vortex and model configurations. They were most sensitive to the vortex size specified in the initial conditions. The larger storm weakened too slowly when moving over land and cool water, and tracked too far to the east over Nova Scotia. Since larger vortices take longer to spin down, the intensity behavior is not surprising. The smaller storm weakened too quickly and tracked too far to the west. Storms of different size would also interact differently with the environment, which could explain the difference in tracks. We discovered that simulations employing the Kuo convective parameterization on the 12-km grid yielded better intensity and track results than Fritsch–Chappel and Kain–Fritsch schemes. We also experimented with the vertical resolution in the model, with the main improvement being on the wind field using higher resolution with more computational levels in the atmospheric BL.

We analyzed the vertical structure of the wind field in the BL over the cool waters of the Scotian Shelf. The wind shear was strong below the low-level jet in the high wind region of the storm, comparing well with observations. The height of the low-level wind jet was

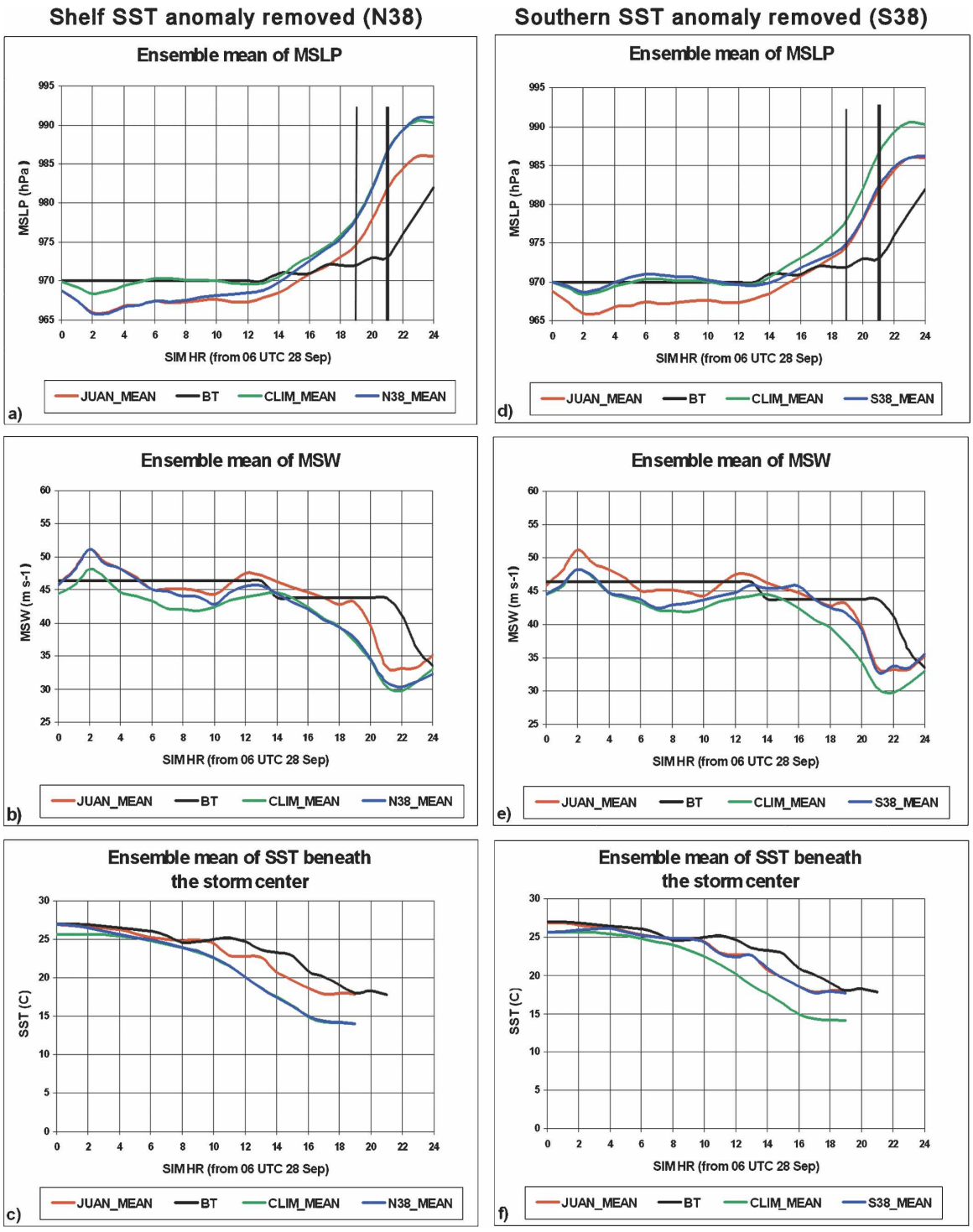

FIG. 15. Time traces of six-member (plus control) subensemble means for the simulations where the shelf SST anomaly is removed (blue curves, N38) on the left-hand side, and where the southern SST anomaly is removed (blue curves, S38) on the right-hand side, compared with subensemble means from the JUAN (red) and CLIM (green) groups with the BT (black). N38: (a) MSLP, (b) MSW, and (c) SST beneath the storm center; (d), (e), (f) same as (a)–(c) except for S38. Mean of simulated landfall time is indicated in (a) and (d) by the thin vertical line and observed landfall time is indicated by the thick vertical line.

lower (300–400 m) in the high wind region of the CLIM (cooler water) storm than the JUAN storm (500 m) with observed SSTs. However, the magnitude of BL wind shear in the CLIM storm was not significantly different from that of the JUAN storm. The reason being that—along with the weaker surface winds—the low-level jet itself was weaker, since the winds also weakened *above* the surface after encountering the cooler water.

Model output was compared with surface weather data and GPS dropsonde data taken from a research aircraft that flew into the storm just prior to landfall. The model effectively reproduced the deep layer of high winds on the right side of the rapidly moving storm with low-level winds in excess of 60 m s^{-1}. It also simulated thermodynamic structures (as denoted by θ_e) in the storm rather well, but overestimated the θ_e overall. The horizontal structure of the wind field at landfall was reproduced quite accurately with the area of maximum winds striking Halifax, Nova Scotia, and areas to the east. The radius of maximum winds in the control simulation was near 45 km compared with an estimate of 35 km based on wind damage patterns.

Two distinct warm SST anomalies (a southern one and a northern one) played a role on the intensity of Juan. The role of each anomaly was investigated separately by removing one from the analysis while retaining the other. Ensembles were run for initial time at 0000 UTC 28 September while single control runs were run for initial time at 0000 UTC 27 September (not shown). It was found that as the storm moved over the continental shelf waters, it began to transition from a climatological state to an anomalous state when only the northern warm SST anomaly was retained. For the simulations starting on 28 September, the storm was as intense as the JUAN control simulation at landfall, implying that the southern SST anomaly made little difference in landfall intensity. *However*, when starting the model on 27 September, the landfall intensity was midway between that of the CLIM and JUAN experiments, implying that the SST anomalies made an equal contribution to the landfall intensity. The latter conclusion is more realistic for we diagnose the SST influence over a greater period of the storm's life cycle.

In the future we wish to expand this work to study storms from previous years for which we have aircraft data with which to validate the model. We have already conducted trial experiments with Hurricane Karen (2001) and Hurricane Michael (2000) with significant improvement over the operational numerical predictions.

Acknowledgments. We thank those who helped set up the modeling system and for technical support throughout the course of this project. They include Serge Desjardins, Ron McTaggart-Cowan, Mike Casey, Weiqing Zhang, Stephane Chamberland, Yves Chartier, Michel Desgagne, Pierre Pellerin, Bruce Brasnett, and Rick Danielson. This project has received funding from the Meteorological Service of Canada (MSC), the NSERC/MARTEC/MSC Industrial Research Chair, and a project grant from the Canadian Foundation for Climate and Atmospheric Sciences. We are also grateful to the MSC for providing access to the supercomputer facility in Dorval, Quebec, where the model runs were carried out and to the National Research Council in partnership with MSC for collection of the aircraft data used in this study.

REFERENCES

Abraham, J., J. W. Strapp, C. Fogarty, and M. Wolde, 2004: Extratropical transition of Hurricane Michael: An aircraft investigation. *Bull. Amer. Meteor. Soc.,* **85,** 1323–1339.

Avila, L. A., 2003: Tropical cyclone report for Hurricane Juan: 24–29 September 2003. NCEP Report, 14 pp. [Available online at http://www.nhc.noaa.gov/2003juan.shtml.]

Benoit, R., J. Cote, and J. Mailhot, 1989: Inclusion of a TKE boundary layer parameterization in the Canadian regional finite-element model. *Mon. Wea. Rev.,* **117,** 1726–1750.

——, M. Desgagné, P. Pellerin, S. Pellerin, S. Desjardins, and Y. Chartier, 1997: The Canadian MC2: A semi-Lagrangian, semi-implicit wide-band atmospheric model suited for fine-scale process studies and simulation. *Mon. Wea. Rev.,* **125,** 2382–2415.

Bolton, D., 1980: The computation of equivalent potential temperature. *Mon. Wea. Rev.,* **108,** 1046–1053.

Chouinard, C., J. Mailhot, H. L. Mitchell, A. Staniforth, and R. Hogue, 1994: The Canadian regional data assimilation system: Operational and research applications. *Mon. Wea. Rev.,* **122,** 1306–1325.

Davidson, N. E., J. Wadsley, K. Puri, K. Kurihara, and M. Ueno, 1993: Implementation of the JMA typhoon bogus in the BMRC tropical prediction system. *J. Meteor. Soc. Japan,* **71,** 437–467.

DeMaria, M., and J. Kaplan, 1994: Sea surface temperature and the maximum intensity of Atlantic tropical cyclones. *J. Climate,* **7,** 1324–1334.

Emanuel, K. A., 1988: The maximum intensity of hurricanes. *J. Atmos. Sci.,* **45,** 1143–1155.

——, C. DesAutels, C. Holloway, and R. Korty, 2004: Environmental control of tropical cyclone intensity. *J. Atmos. Sci.,* **61,** 843–858.

Evans, J. L., 1993: Sensitivity of tropical cyclone intensity to sea surface temperature. *J. Climate,* **6,** 1133–1140.

Franklin, J. L., M. L. Black, and K. Valde, 2003: GPS dropwindsonde wind profiles in hurricanes and their operational implications. *Wea. Forecasting,* **18,** 32–44.

Fritsch, J. M., and C. F. Chappel, 1980: Numerical prediction of convectively driven mesoscale pressure systems. Part I: Convective parameterization. *J. Atmos. Sci.,* **37,** 1722–1733.

Fujita, T., 1952: Pressure distribution within a typhoon. *Geophys. Mag.,* **23,** 437–451.

Gal-Chen, T., and R. Somerville, 1975: On the use of a coordinate

transformation for the solution of the Navier-Stokes equations. *J. Comput. Phys.,* **17** (2), 209–228.

Geshelin, Y., J. Sheng, and R. J. Greatbatch, 1999: Monthly mean climatologies of temperature and salinity in the western North Atlantic. Canadian Tech. Rep. of Hydrography and Ocean Sciences, 153, 62 pp.

Jones, S. C., and Coauthors, 2003: The extratropical transition of tropical cyclones: Forecast challenges, current understanding, and future directions. *Wea. Forecasting,* **18,** 1052–1092.

Kain, J. S., and J. M. Fritsch, 1990: A one-dimensional entraining/detraining plume model and its application in convective parameterization. *J. Atmos. Sci.,* **47,** 2784–2802.

Kuo, H. L., 1974: Further studies on the parameterization of the influence of cumulus convection on large-scale flow. *J. Atmos. Sci.,* **31,** 1232–1240.

Malkin, W., and G. C. Holzworth, 1954: Hurricane Edna, 1954. *Mon. Wea. Rev.,* **82,** 267–279.

McTaggart-Cowan, R., E. Atallah, J. R. Gyakum, and L. F. Bosart, 2006a: Hurricane Juan (2003). Part I: A diagnostic and compositing life cycle study. *Mon. Wea. Rev.,* in press.

——, ——, ——, and ——, 2006b: Hurricane Juan (2003). Part II: Forecasting and numerical simulation. *Mon. Wea. Rev.,* in press.

Price, J. F., 1981: Upper ocean response to a hurricane. *J. Phys. Oceanogr.,* **11,** 153–175.

Schade, L. R., 2000: Tropical cyclone intensity and sea surface temperature. *J. Atmos. Sci.,* **57,** 3122–3130.

Shearman, R. J., 1989: The mathematical representation of wind profiles over the sea. WMO/Tech. Doc. 311, 7 pp.

Simpson, R. H., and H. Riehl, 1981: *The Hurricane and Its Impact.* Louisiana State University Press, 398 pp.

Stull, R. B., 1988: *An Introduction to Boundary Layer Meteorology*. Kluwer Academic, 666 pp.